Journal of Ceramic Processing Research. Vol. 15, No. 4, pp. 231~235 (2014)

J O U R N A L O F
Ceramic Processing Research

Microstructure and mechanical properties of ultra fine grained TiC-Nicrobraz hard materials fabricated by a high frequency induction heated sintering

Kee-Do Woo*, Duck-Soo Kang and In-Jin Shon
Division of Advanced Materials Engineering and RCAMD, Chonbuk National University, Chonbuk 561-756, Korea

The ultra fine grained TiC-10 vol.% binders (Nicrobraz 30, 150 and LC) hard materials were fabricated successfully by a high-frequency induction heated sintering (HFIHS) using high-energy mechanical ball milled TiC powder. The average grain size of high energy mechanical ball milled TiC powder was approximately 50 nm. TiC-Nicrobraz (30, 150, LC) hard materials with a relative density of up 99% were obtained by HFIHS. The hardness and fracture toughness of the sintered TiC-10 vol% Nicrobraz 30 hard materials produced by HFIHS were 2018.7 kg/mm^2 and 8.2 MPa · m$^{1/2}$, respectively.

Key words: TiC, Nanocomposite, Milling, Sintering, Hardness, Fracture toughness.

Introduction

In recent years, TiC-powders have been widely used as reinforcements in metal matrix composites (MMCs) to improve the mechanical properties [1]. TiC-based hard materials are subjected to extensive research efforts to develop applications in cutting tool, roller and cermet materials due to their many attractive properties, such as high hardness, high melting temperature, high elastic modulus and electrical conductivity [2-3]. Generally, TiC-based hard materials were fabricated with addition of binder, such as Co [4]. However, the high cost of Co binder is replaced by nickel or iron in order to provide better performance in tribo-systems to be corrosive [5]. For over 50 years, Nicrobraz (Ni-Cr based powder) has represented the pioneers in high-temperature brazing. Nicrobraz has more economical binder than Co binder. Also this binder is better corrosion resistance than Co, Ni and Fe-binders.

Powder metallurgy (PM) is favorable process for synthesizing ultrafine grained TiC based hard materials. PM allows the use of nanostructures or ultrafine structured powders and nanopowder produced using various processes such as high energy mechanical ball milling (HEBM) and rapid solidification [6]. HEBM method has not only useful technique for synthesizing metals-ceramics compounds but also fabrication of ultra fine grain composites [7]. However, the grain size of sintered materials becomes much larger than that in pre-sintered powders due to a fast grain growth during the conventional sintering process. So, controlling grain growth during sintering is one of the keys to the commercial success of ultra fine grain hard materials. High frequency induction heated sintering can be control the grain growth during sintering at low temperature for a short time [8]. Also, high density of composites could be obtained by HFIHS.

The object of this study is to produce high densification and ultra fine TiC-10 vol.% Nicrobraz 30, 150, LC hard materials in very short sintering times at low temperature and investigate binder effect of the sintered specimens by HFIHS using HEBM powders.

Experimental Procedure

The TiC powder (99.5% pure, particle size < 2 μm) used in this study was supplied by Alfa. Composition of Nicrobraz 30, 150 and LC (99.1% pure, particle size < 10 μm) as binders are shown in Table 1. TiC powder was placed into a hardened steel vial, together with tungsten balls. And ball to powder weight ratio was 30 : 1. The vial was then sealed in a glove-box filled with high purity argon. The TiC powders were first milled in a high-energy ball mill (Pulverisette-5 planetary mill) at 250 rpm for 10 h. The size of milled TiC powders was calculated from the full-width at half maximum (FWHM) using equation of the Suryanarayana and Norton [9].

Table 1. The compositions of Nicrobraz 30, 150 and LC (at.%).

	Cr	Si	B	Fe	C	Ni
Nicrobraz 30	19.0	10.2	–	–	0.06	Bal.
Nicrobraz 150	15.0	–	3.5	–	0.06	Bal.
Nicrobraz LC	14.0	4.5	3.0	4.5	0.06	Bal.

*Corresponding author:
Tel : +82-63-270-2299
Fax: +82-63-270-2305
E-mail: kdwoo@jbnu.ac.kr

$$B_r(B_{crystalline} + B_{strain})\cos\theta = K\lambda/L + \eta\sin\theta \quad (1)$$

where B_r is the FWHM of the diffraction peak after instrument correction; $B_{crystalline}$ and B_{strain} are FWHM caused by small grain size and internal stress, respectively; k is a constant (with a value of 0.9); λ is the wavelength of the X-ray radiation; L and η are grain size and internal strain, respectively; θ is the Bragg angle. The parameters B and B_r follow Cauchy's form with the relationship: $B = B_r + B_s$, where B and B_s are FWHM of the broadened Bragg peaks and the standard sample's Bragg peaks, respectively.

The TiC-10 vol.% Nicrobraz 30, 150 and LC powders were mixed at horizontal rotation velocity of 150 rpm for 24 h with ceramic balls to powder weight ratio of 6 : 1. The mixed powders were observed by field emission-scanning electron microscope (FE-SEM) and transmission electron microscopy (TEM). The mixed TiC-10 vol.% Nicrobraz 30, 150 and LC powders were placed in a graphite die (outside diameter: 45 mm, inside diameter: 10 mm, height: 40 mm) and then introduced into the HFIHS apparatus (Eltek Co., Republic of Korea) [8, 10, 11]. To prevent reaction between sintered composite and graphite die, BN was coated inside of graphite die. The chamber was first evacuated down to 10^{-3} torr and a uniaxial pressure of 80 MPa was applied. An induced current was then activated and maintained until the densification rate was negligible, as indicated by the observed shrinkage of the sample. The composites shrinkage and temperature were measured by using a linear gauge that measured the vertical displacement and the pyrometer focused on the surface of the graphite die, respectively. The heating rate was approximately 600 ºC/min in the process. At the end of the process, the induced current was turned off and the composites were allowed to cool to room temperature. The relative density of sintered composites was calculated by Archimedes principle. The phase analysis of sintered composites was investigated by XRD. And the hardness and fracture toughness were measured using the Vickers's hardness at load of 20 kgf for 15s. Indentations with large enough loads produced radial cracks emanating from the corners of the indent. The length of these cracks permits an estimation of the fracture toughness of the material by means of the Anstis et al. expression [12].

$$K_{IC} = 0.016(E/H)^{1/2}P/C^{3/2} \quad (2)$$

Where E, H, P and C is Young's modulus, the indentation hardness, the indentation load, and the trace length of the crack measured from the center of the indentation, respectively. Typically, one to three additional cracks were observed to propagate radically from the indentation. In the same manner as hardness values, the toughness values were derived from the average of ten measurements. The sintered composites were etched by Murakami's solution for 2 min at room temperature. The surface of etched specimen was observed by FE-SEM with energy dispersive spectroscopy (EDS).

Results and Discussion

Size and morphology of HEBM powders

The SEM images of raw and 10 h-milled TiC powders are presented in Fig. 1. TiC powder without milling has an angular shape, but the 10h-milled TiC powder has a round shape and refinement with milling time. The size of 10 h-milled powder is about 50 nm measured by FWHM of XRD results of Fig. 2. The FWHM of XRD patterns of the milled powder was wider than that of the raw powder due to internal strain and a decrease in grain size. This means that size of 10 h milled powder is finer than raw TiC powder. The shape of Nicrobraz powders is round type and the average size of these powders is about 10 μm. The TEM images of milled TiC-10 vol.% Nicrobraz LC powders were shown in Fig. 3. In bright field image (a) and dark field image (b), the milled powders were refined by HEBM. In dark field image, white phases represent TiC milled particles. Also, The SADP (c)

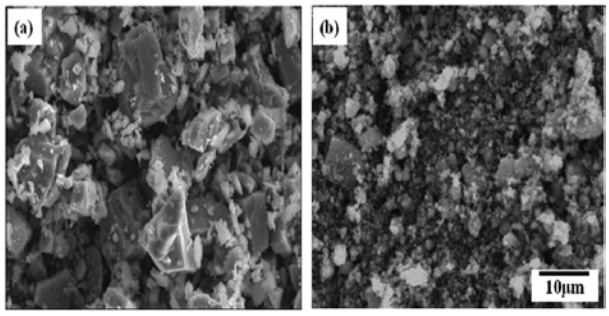

Fig. 1. SEM images of the TiC powders: (a) raw TiC powders and (b) 10 h milled powders.

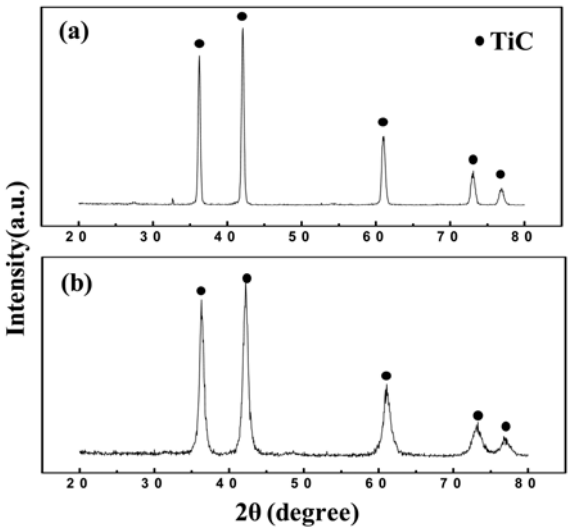

Fig. 2. XRD patterns of TiC: (a) raw powder (b) 10 hr milled powder.

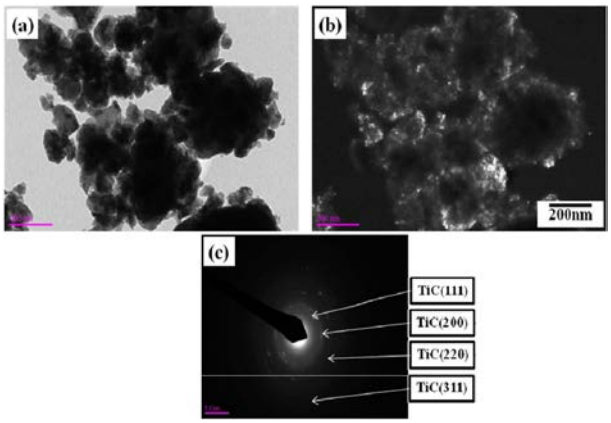

Fig. 3. TEM images of the milled TiC-10 vol.% Nicrobraz LC powders: (a) BFI, (b) DFI and (c) SADP.

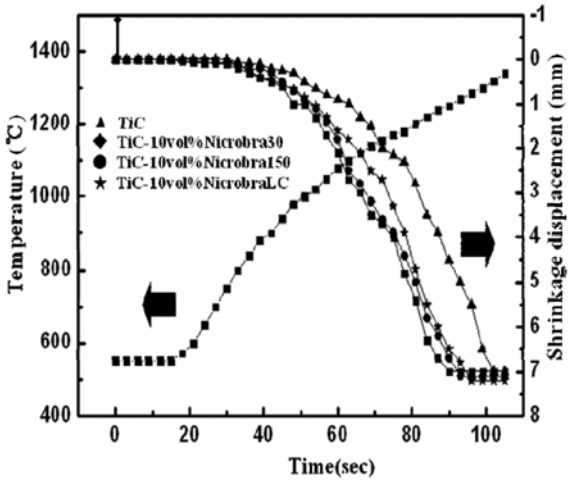

Fig. 4. Variations of temperature and shrinkage displacement with heating time during the sintering of the 10 h milled TiC-10 vol.% Nicrobraz (30, 150, LC) powder by HFIHS.

shows ring pattern due to ultra fine particle during ball milling process [13, 14]. The final powder mixtures consist of nano-sized TiC particles and micronized Nicrobraz elements.

Densification behavior and microstructures

Fig. 4 shows the change in shrinkage and temperature with the heating time during the sintering of 10 h milled TiC-10 vol.% Nicrobraz 30, 150, LC specimens and raw TiC without binder by HFIHS under 80 MPa pressure. The sintering temperature of 10 h milled TiC-10 vol.% Nicrobraz 30, 150 and LC specimens was at approximately 1200 ºC, because the densification rate became almost negligible. But the sintering temperature of raw TiC powder was at 1300 ºC This is because decreasing of sintering temperature due to higher free surface and surface volume energy obtained by HEBM. The main densification mechanism involves the rearrangement of carbide particle, enhancement of diffusion, and viscous flow of the binder [15].

Fig. 5 shows XRD patterns of sintered TiC-10 vol.% Nicrobraz 30, 150 and LC specimens. TiC peaks were

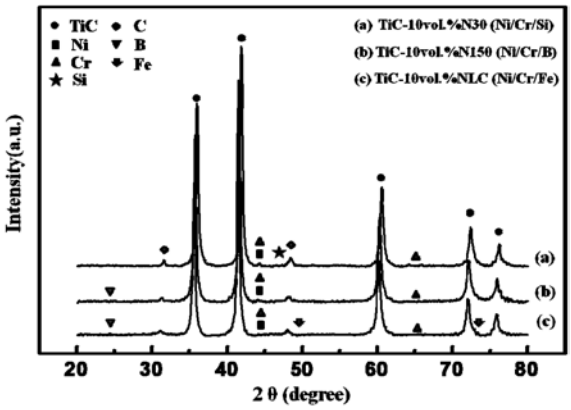

Fig. 5. XRD patterns of the sintered TiC-10 vol.% Nicrobraz hard materials (30, 150, NLC) by HFIHS using 10 h milled powders: (a) Nicrobraz 30, (b) Nicrobraz 150 and (c) Nicrobraz LC.

largely detected. However, Nicrobraz elements peaks rarely were indicated. Because it is deduced that amount of binders was smaller than TiC, relatively. While the sintering is being conducted, both TiC and binders didn't make new phases. The average grain sizes of the sintered TiC-10 vol.% Nicrobraz 30, 150 and LC specimens were determined to be approximately 62 nm, 65 nm and 75 nm, respectively, calculated by Suryanarayana and Norton equation [9]. From this result, the grain growth was not occurred because of shorter sintering time at lower temperature than commercial sintering method.

The back scattered electron images of the etched TiC-10 vol.% Nicrobraz 30, 150 and LC specimens were shown in Fig. 6. The gray or dark phase is the TiC-rich (A) phase, TiC phase (B) and the white phase (C) is the Nicrobraz-rich phase. It is shown that the Nicrobraz phases are distributed between the TiC particles and solid soluted in TiC phase. The surface of the binderless sintered TiC hard material using raw TiC particle exists many pore (Fig 6(a)). But a few pore can be seen that the sintered TiC-10 vol.% Nicrobraz 30, 150 and LC specimens using HEBM powders with binder (Fig. 6(b), (c) and (d)). For these results, high relative density (about 99%) of ultra fine grained hard materials can be fabricated successfully by HFIHS using HEBM powder with binder (Table 2). But in this SEM image, grain size of sintered composite showed micro-sized grains. This result didn't coincident with XRD results. Therefore , high resolution SEM image of grain was needed to observe nano-sized grain. To clarify the nano-sized particles calculated by XRD peak, FE-SEM was used. In Fig. 6(e) of FE-SEM image, high resolution FE-SEM micrograph showed many nano-sized grains in one micro-sized TiC grain of the sintered hard material. This is because one big particle in Fig. 1(b) contains many nano-sized particles. By rapid sintering, these nano-sized particles couldn't grow rapidly. Therefore, nano-sized grains of the sintered hard material were fabricated by HFIHS with high energy ball milled powder.

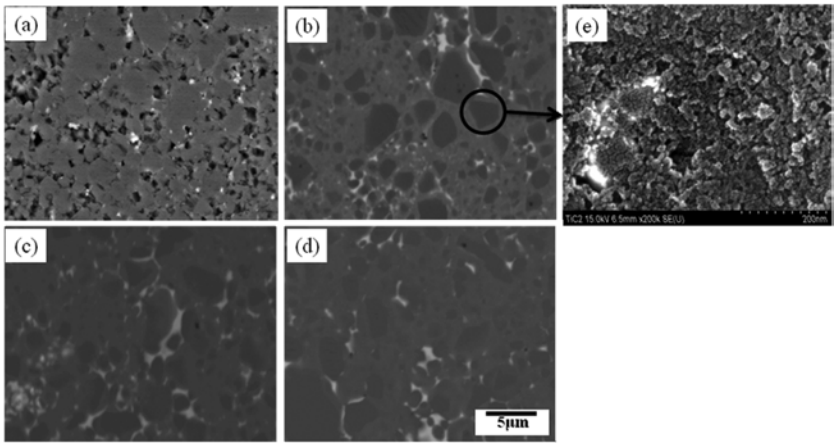

Fig. 6. Back scattered electron images of the sintered hard materials produced by HFIHS using 10 h milled powders: (a) TiC, (b) TiC-10 vol.% Nicrobraz 30, (c) TiC-10 vol.% Nicrobraz 150, (d) TiC-10 vol.% Nicrobraz LC and (e) nano-sized TIC particles of the sintered TiC-10 vol.% Nicrobraz 30 by FE-SEM.

Table 2. Physical and mechanical properties of specimens.

	Relative Density (%)	Hardness (kg/mm^2)	Fracture Toughness ($MPa \cdot m^{1/2}$)	Grain Size (nm)
Binderless TiC	96.1	1553.3	6.2	94
TiC-10 vol.%N30	99.3	2018.7	8.2	62
TiC-10 vol.%N150	99.3	2005.5	8.3	65
TiC-10 vol.%NLC	98.8	1994.1	8.6	75

Physical and mechanical properties

The Vickers hardness and fracture toughness of the sintered TiC-10 vol.% Nicrobraz 30, 150, LC specimens were shown in Table 2. The measured Vickers hardness of raw TiC, 10 h-milled TiC-10 vol.% Nicrobraz 30, 150 and LC specimens produced by HFIHS were 1553.3 kg/mm^2, 2018.7 kg/mm^2, 2005.5 kg/mm^2 and 1994.1 kg/mm^2, and fracture toughness were 6.2 $MPa \cdot m^{1/2}$, 8.2 $MPa \cdot m^{1/2}$, 8.3 $MPa \cdot m^{1/2}$ and 8.6 $MPa \cdot m^{1/2}$, respectively. Hardness of binder added TiC hard materials increased due to refinement of microstructure. In accordance with the Hall-Petch relationship [16-17], the hardness of hard materials increases with a decrease in grain size. But there were a few differences in fracture toughness between the three binders added TiC hard materials. This is due to different particle sizes and different binders. The hardness of TiC-10 vol.% Nicrobraz LC specimen is very high rather than that of WC-6%Co (Hv: 1580), but fracture toughness is little lower than that of WC-6%Co hard material (K_{1C}: 9.6 $MPa \cdot m^{1/2}$) [18].

Summary

TiC-based hard materials are useful materials for cutting tool and roller. Therefore, cheap and improved mechanical properties of TiC based hard materials are needed to be developed. Nicrobraz 30, 150, LC are cheaper binder than Co and Ni in TiC hard materials.

To improve the mechanical property, high densification and ultra fine grain TiC-10 vol.% Nicrobraz 30, 150, LC hard materials should be developed by rapid sintering using nano-sized powders.

Nano-sized TiC powder can be obtained by HEBM for 10h. The rapid consolidation of TiC- 10 vol.% Nicrobraz 30, 150 and LC hard materials can be obtained by HFIHS using the 10 h-HEBM powder. These nano-sized TiC particles showed excellent sinterablity. Fully densed TiC-10 vol.% Nicrobraz 30, 150, LC hard materials could be obtained within 2 min at 1200 ºC The hardness of binderless TiC, 10 h-milled TiC-10 vol.% Nicrobraz 30, 150 and LC hard materials produced by HFIHS were 1553.3 kg/mm^2, 2018.7kg/mm^2, 2005.5 kg/mm^2 and 1994.1 kg/mm^2, and fracture toughness were 6.2 $MPa \cdot m^{1/2}$, 8.2 $MPa \cdot m^{1/2}$, 8.3 $MPa \cdot m^{1/2}$ and 8.6 $MPa \cdot m^{1/2}$, respectively. Hardness, toughness and sintering efficiency of TiC hard materials were improved by nano-sized particles with binder (Nicrobraz 30, 150 and LC) addition.

The hardness of TiC-10 vol.% Nicrobraz 30, 150 and LC hard materials is very high rather than WC-Co hard material.

References

1. B. Li, Y. Liu, H. Cao, L. He, J. Li, Mater. Let. 63 (2009) 2010-2012.
2. B. J. Choi, Y. J. Kim, Kor. J. Met. Mater. 48 [8] (2010)

780-789.
3. K. D. Woo, B. R. Kim, E. P. Kwon, D. S. Kang, I. J. Shon, Ceram. Int. 36 (2010) 351-355.
4. K. Mohan, P. R. Strutt, Nanostruct. Mater. 7 (1996) 547-555.
5. S. G. Shin, J. H. Lee, Met. Mater. Int. 12 [1] (2006) 57-62.
6. Y. Y Chen, H. B. Yu, D. L. Zhang, L. H. Chai, Mater. Sci. Eng. A 525 (2009) 166-173.
7. D. L. Zhang, Pro. Mater. Sci. 49 (2004) 537-560.
8. H. C. Kim, I. J. Shon, Z. A. Munir, J. Mater. Sci. 40 (2005) 2849-2854.
9. C. Suryanarayana, M. Grant Norton, X-ray Diffraction :A Practical Approach, Plenum Press, New York, (1988) 207-213.
10. In-Jin Shon, In-Kyoon Jeong, In-Yong Ko, Jung-Mann Doh, Kee-Do Woo, Ceramics Inter., 35 (2009) 339-344.
11. H.C. Kim, I.J. Shon, I. Y. Ko, J. K. Yoon, J. M. Doh, Met. Mater. Int. 13 (2007) 39-46.
12. GR Anstis, P Chantikul, BR Lawn, DB Marshall, J. Am. Ceram. Soc, 1981, 64 (9), 533-538.
13. M. Sherif El-Eskanadarany, J. Alloys Compd. 305 (2000), 225-238.
14. Y. F. Zhang, L. J. Wang, W. Jiang, L. Chen, G. Z. Bai, J. Europ. Ceram. Soc. 26 (2006) 3393-3397.
15. G.S. Upadhyaya, Mater. Des. 22 (2001) 483-489.
16. H.O. Hall, Proc. Phys. Soc. B 64 (1951) 747-753.
17. N. J. Petch, J. Iron Steel Inst. 174 (1953) 25-28.
18. European powder metallurgy association, Powder Metallurgy of Hardmaterials, Introduction, Shrewsbury, England (1995) 16/17.